Supplementary Information

Table of Content

Table S1. Sample information in DS1. 3

Table S2. Sample information in DS2. 4

Table S3. Numbers of sequence reads. 5

Table S4. Mismatch counts in the mapped reads. 6

Table S5. Overlap of segments showing age-related splicing changes in DS1 and DS2. 7

Table S6. PCR validation of age-related splicing changes. 8

Table S7. Rhesus macaque sample and sequence read coverage information. 10

Table S8. Functional characteristics of genes in different splicing patterns. 11

Table S9. List of correlated splicing factors. 12

Table S10. Enrichment of genes with cell-type specific expression in splicing patterns (top) or brain region-specific genes (bottom). 13

Table S11. Splicing factor binding motifs. 14

Table S12. PCR primers. 15

Figure S1. The distribution and frequency of mismatches along reads. 16

Figure S2. Effect of allowing mismatches during read mapping on inclusion ratio changes with age. 17

Figure S3. Effect of allowing mismatches during read mapping on changes in intron retention with age. 18

Figure S4. Retention of the 7th intron of the *AKR1B1* gene. 19

Figure S5. The distribution of read overhangs lengths spanning splice junctions. 20

Figure S6. Correlation between age-related inclusion ratio changes measured by Affymetrix Exon Arrays and RNA-seq. 21

Figure S7. Inclusion ratio change index distribution for gene segments showing significant inclusion ratio change in development and/or aging. 22

Figure S8. Scatter plot of splicing change index distribution containing splicing type information. 23

Figure S9. For major age-related splicing change patterns in the human and macaque PFC. 24

Figure S10. Relationship between gene expression and segment inclusion ratio. 26

Figure S11. Hierarchical clustering of inclusion ratio values reveals distinct splicing patterns. 27

Figure S12. Correlation of differences in age-related splicing changes between PFC and CBC measured using RNA-seq and Affymetrix Exon Arrays. 28

Figure S13. Alternative splicing of *APP* exon 9..... 29

Figure S14. Alternative splicing of the 6th exon of the *BIN1* gene. 30

Figure S15. Multi-dimensional scaling (MDS) analysis of splicing divergence. 31

Figure S16. Age-related splicing changes in African-Americans and Caucasians. 32

Figure S17. Gene coverage bias. 33

Supplementary tables

Table S1. Sample information in DS1.

Sample ID	Brain Bank ID	Age		Sex	PMI[1]	RIN[2]		Source	Ethnicity	Cause of death
		Years	Days			PFC	CBC			
Pool 1	Maryl_447	0	2	m	3	8	7.2	NICHD[3]	Caucasian	Complications of birth
	Maryl_779	0	5	m	5	8.8	7.8	NICHD	African American	Congenital heart defect
	Maryl_398	0	16	f	3	9.1	8.3	NICHD	African American	Complications of birth
	Maryl_1157	0	20	f	14	7.1	7.5	NICHD	Caucasian	Pneumonia associated with meconium aspiration
	Maryl_759	0	35	m	7	7.9	6.9	NICHD	Caucasian	Idiopathic pulmonary hemorrhage
Pool 2	Maryl_1325	0	182	f	1	8.4	8.1	NICHD	African American	Sudden infant death syndrome
	Maryl_131	0	198	f	24	7.8	7.9	NICHD	Caucasian	Sudden infant death syndrome
	Maryl_1281	0	206	m	6	8.4	7.2	NICHD	African American	Sudden infant death syndrome
	Maryl_121	0	224	m	20	6.7	6.8	NICHD	Caucasian	Sudden infant death syndrome
	Maryl_435	0	274	m	10	7.5	6.2	NICHD	Caucasian	Meningitis
Pool 3	4669	16	125	m	16	8.3	8.2	NICHD	Caucasian	Neck and head injuries
	4848	16	271	m	15	9.1	7.6	NICHD	Caucasian	Accident, drowning
	1409	18	38	m	6	7.2	6.8	NICHD	Caucasian	Accident, multiple injures
	1011	19	69	f	7	6.5	7	NICHD	Caucasian	Accident, multiple injures
	933	20	255	m	12	8.7	8.9	NICHD	Caucasian	Accident, lightning strike
Pool 4	1455	25	149	f	7	7.4	8.1	NICHD	Caucasian	Multiple injures
	605	25	152	m	19	9.2	8.9	NICHD	African American	Asthma
	602	27	42	m	15	8.8	8.9	NICHD	African American	Asthma
	1026	28	131	m	6	8.1	7.5	NICHD	Caucasian	Congenital heart disease
	1365	28	239	m	17	8.2	7.4	NICHD	Caucasian	Accident, multiple injuries
Pool 5	S96/206	70	0	f	11	8	7.6	NBB[4]	Caucasian	Metastasised mamma carcinoma
	4735	73	184	m	21	7.5	6	NICHD	Caucasian	Chronic obstructive pulmonary disease
	S01/322	73	0	f	14	7.6	6.4	NBB	Caucasian	Respiratory insufficiency
	S00/059	78	0	f	7	8.3	7.9	NBB	Caucasian	Dec.cordis
	S04/057	80	0	m	7	8.6	7	NBB	Caucasian	Ventricular fibrillation
Pool 6	S01/118	88	0	m	7	7.7	7.3	NBB	Caucasian	Euthanasia
	S96/297	90	0	f	6	7.8	7.6	NBB	Caucasian	Cardiac arrest
	S03/084	96	0	m	6	7.3	7.1	NBB	Caucasian	Heart failure
	S03/119	97	0	f	5	8.4	8	NBB	Caucasian	Asthma cardialis
	S00/047	98	0	m	9	7.3	7.5	NBB	Caucasian	Bleeding from aorta fissure

[1]*PMI*: Postmortem intervals in hours.
[2]*RIN*: RNA integrity values measured by Agilent Bioanalyzer.
[3]*NICHD*: Brain and Tissue Bank for Developmental Disorders at the University of Maryland, USA.
[4]*NBB*: Netherlands Brain Bank, Amsterdam, Netherlands.
Samples used in both DS1 and DS2 are highlighted in gray.

Table S2. Sample information in DS2.

Brain Bank ID	Age		Sex	PMI[1]	RIN[2]	Source	Ethnicity	Cause of death
	Years	Days						
Maryl_779	0	5	m	5	8.8	NICHD[3]	African American	Congenital heart defect
Maryl_1157	0	20	f	14	7.1	NICHD	Caucasian	Pneumonia associated with meconium aspiration
Maryl_759	0	35	m	7	7.9	NICHD	Caucasian	Idiopathic pulmonary hemorrhage
Maryl_1055	0	94	m	12	7.7	NICHD	Caucasian	Bronchopneumania
Maryl_1281	0	204	m	6	8.4	NICHD	African American	Sudden infant death syndrome
1453	1	78	m	19	7.6	NICHD	African American	Asthma
1275	2	57	f	21	7.5	NICHD	African American	Acute myocarditis
1908	13	360	m	13	8.3	NICHD	Caucasian	Hanging
605	25	152	m	19	9.2	NICHD	African American	Asthma
1496	53	112	m	17	8.3	NICHD	Caucasian	Arteriosclerotic cardiovascular disease
S06/117	66	0	m	10	8.6	NBB[4]	Caucasian	Ruptured abdominal aneurysm aorta
S01/118	88	0	m	7	7.7	NBB	Caucasian	Euthanasia
S00/047	98	0	m	9	7.3	NBB	Caucasian	Bleeding from aorta fissure

[1]*PMI*: Postmortem intervals in hours.
[2]*RIN*: RNA integrity values measured by Agilent Bioanalyzer.
[3]*NICHD*: Brain and Tissue Bank for Developmental Disorders at the University of Maryland, USA.
[4]*NBB*: Netherlands Brain Bank, Amsterdam, Netherlands.
Samples used in both DS1 and DS2 are highlighted in gray.

Table S3. Numbers of sequence reads.

Dataset	Sample ID / Brain Bank ID	Brain Region	Total read pairs (DS2 – reads)	Mapped read pairs (DS2 – reads)	Location of mapped reads		
					gene	exon	junction
1	Pool 1	PFC	12986849	8394381	7732954	6309623	1571150
	Pool 1	CBC	14401087	9183265	8449786	6487468	1827020
	Pool 2	PFC	18606331	10064574	9255556	7650490	1713418
	Pool 2	CBC	17173882	9962309	9123172	6740399	1769939
	Pool 3	PFC	10867452	7114384	6665929	5882014	1717835
	Pool 3	CBC	11454526	7401286	6851346	5359984	1662481
	Pool 4	PFC	17660808	10543725	9912871	8528704	2786008
	Pool 4	CBC	16720362	10467977	9669924	7396281	2316290
	Pool 5	PFC	17715490	9821954	9162963	7645879	1895665
	Pool 5	CBC	17130871	10443253	9547717	7116620	1941140
	Pool 6	PFC	14164681	8710121	8159383	7019562	1977553
	Pool 6	CBC	12673390	7691734	7071345	5452222	1507773
2	Maryl_779	PFC	21284713	14379727	13204850	10882306	3570100
	Maryl_1157	PFC	20754409	11843993	10746223	8779519	2331123
	Maryl_759	PFC	23722421	16285468	15044787	12824078	4379569
	Maryl_1055	PFC	23416250	15119297	13889701	11883054	3065203
	Maryl_1281	PFC	22698303	14764891	13592458	11845774	3340220
	1453	PFC	23934412	16143315	14975097	13250399	4420759
	1275	PFC	17759057	11401664	10508629	9195223	2870504
	1908	PFC	19901399	12479373	11676044	10643369	3348264
	605	PFC	23201284	15203403	14242124	12877188	4312333
	1496	PFC	16019209	10396263	9721112	8784880	2732116
	S06/117	PFC	20948595	14199806	13281513	11742463	3947097
	S01/118	PFC	21032459	14104142	13108149	11366346	3502188
	S00/047	PFC	20255260	13994072	13069914	11391485	3564658
Total			477761149	180315414	167060601	145466084	45384134

Table S4. Mismatch counts in the mapped reads.

Dataset	ID	Brain region	Mismatch count			
			0	1	2	3
1	Pool 1	PFC	0.64	0.25	0.07	0.03
	Pool 1	CBC	0.6	0.27	0.09	0.03
	Pool 2	PFC	0.57	0.28	0.1	0.05
	Pool 2	CBC	0.53	0.29	0.12	0.05
	Pool 3	PFC	0.64	0.25	0.08	0.03
	Pool 3	CBC	0.61	0.25	0.1	0.05
	Pool 4	PFC	0.6	0.25	0.1	0.05
	Pool 4	CBC	0.59	0.26	0.1	0.05
	Pool 5	PFC	0.64	0.25	0.08	0.03
	Pool 5	CBC	0.57	0.28	0.1	0.04
	Pool 6	PFC	0.54	0.28	0.12	0.06
	Pool 6	CBC	0.51	0.3	0.13	0.06
2	Maryl_779	PFC	0.71	0.18	0.07	0.04
	Maryl_1157	PFC	0.72	0.17	0.07	0.04
	Maryl_759	PFC	0.67	0.21	0.07	0.04
	Maryl_1055	PFC	0.73	0.17	0.06	0.04
	Maryl_1281	PFC	0.70	0.18	0.07	0.04
	1453	PFC	0.69	0.21	0.06	0.03
	1275	PFC	0.72	0.19	0.06	0.03
	1908	PFC	0.72	0.19	0.06	0.03
	605	PFC	0.70	0.21	0.06	0.03
	1496	PFC	0.75	0.17	0.05	0.03
	S06/117	PFC	0.76	0.16	0.05	0.03
	S01/118	PFC	0.76	0.16	0.05	0.03
	S00/047	PFC	0.77	0.16	0.05	0.03

Table S5. Overlap of segments showing age-related splicing changes in DS1 and DS2.

	DS1	DS2	Shared	*p*-value[1]
Segments	3,132	6,114	1,484	$<1\times10^{-50}$
Gene	1,456	2,588	721	$<1\times10^{-20}$

[1]Excess of the significant age-related splicing changes overlapping between DS1 and DS2 was tested using Fisher's exact test. The significance analysis was based on 30,122 segments (from 6,758 genes) with sufficient sequence reads coverage in both datasets.

Table S6. PCR validation of age-related splicing changes.

Seg	AGAP3			AKR1B1			ASPH		CADPS		CDC42BPA	
Pos[1]	34157-37048			11261-11987			181884-181928		83378-83510		21014-21199	
Age[2]	1	3	5	1	4	5	5	3	1	6	6	1
Seq[3]	.205	.441	.533	.471	.089	.231	.602	.907	.261	.749	.581	0
PCR[4]	.145	.388	.424	.220	.082	.093	.670	.905	.254	.805	.345	.039
Gel[5]												

Seg	CTNNA2		DBN1		DCLK1		EXD3			FMNL2		
Pos	1433854-1433997		2996-3133		19228-19301		56722-66995			305555-313054		
Age	1	6	1	3	1	6	1	3	5	1	4	6
Seq	.348	.023	.270	.923	.060	.482	.943	.399	.151	.916	.257	.397
PCR	.394	.146	.190	.808	.175	.707	.261	.058	.090	.813	.378	.294
Gel												

Seg	GRIN1		LMO7		MAPRE3		MAPT			MAPT		
Pos	9763-9825		234827-234935		53642-53686		77476-77535			115927-116019		
Age	4	1	6	1	1	4	4	1	2	2	4	1
Seq	.267	.043	.641	.012	.296	.802	.429	.083	.019	.327	.457	.056
PCR	.262	.051	.559	.188	.301	.858	.268	0	0	.312	.518	.021
Gel												

Seg	MATR3			NDRG2		NEO1			NRCAM		PALM	
Pos	51545-51688			6102-6143		240857-241015			78008-78064		31400-31531	
Age	4	3	2	2	4	3	2	5	3	2	1	5
Seq	.177	.286	.460	.311	.513	.434	.380	.841	.255	.792	.059	.397
PCR	.191	.198	.284	.201	.613	.429	.396	.661	.245	.792	.012	.436
Gel												

Seg	R3HDM1			SGIP1		UBP1[6]			WNK1	
Pos	73402-90154			148487-148911		47918-48809			126651-127109	
Age	5	4	1	1	3	1	4	6	5	1
Seq	1	.930	.455	.036	.765	.542	.177	.063	.176	.771
PCR	.740	.895	.298	.046	.785	.340	.099	.102	.023	.673
Gel										

[1]*Pos*: the relative position of the segment counted from the 5' end of the gene.

[2]*Age* 1 to 6 denote youngest to oldest samples (PFC from DS1) respectively.

[3]*Seq*: the inclusion ratio calculated by RNA-seq DS1.

[4]*PCR*: the inclusion ratio calculated by RT-PCR.

[5]*Gel*: the PCR gel image.

[6]*UBP1* is a test of age-related intron retention.

Table S7. Rhesus macaque sample and sequence read coverage information.

Brain Bank ID	Age		Sex	RIN[1]	Source	Total number of reads	Number of mapped reads
	Years	Days					
NB0902	0	1	m	8.9	SEAC[2]	35,647,306	25,827,729
NB0901	0	1	m	8.3	SEAC	36,207,576	24,083,109
NB0905	0	7	m	8.7	SEAC	35,368,530	23,638,865
0705	0	16	m	9.1	SEAC	33,944,540	23,157,558
0703	0	22	m	9.9	SEAC	35,150,179	22,902,814
070141	0	153	m	9.3	SEAC	36,074,539	23,601,772
070133	0	207	m	9.1	SEAC	34,525,819	23,390,434
06711	0	310	m	9.8	SEAC	31,005,239	19,386,532
051095	2	9	m	9.5	SEAC	32,143,377	18,674,467
03071	4	27	m	9.7	SEAC	30,998,685	18,332,895
98073	9	104	m	9	SEAC	32,106,698	19,123,960
92107	15	3	m	9.5	SEAC	31,450,483	19,056,475
85091	22	74	m	9.2	SEAC	28,942,443	17,622,622
198100	26	28	m	8.6	SEAC	29,315,091	17,111,572
QDL II	28	0	f	7.8	SEAC	29,042,277	16,679,686

[1]*RIN*: RNA integrity values measured by Agilent Bioanalyzer.
[2]*SEAC*: Suzhou Experimental Animal Center, Suzhou, China.

Table S8. Functional characteristics of genes in different splicing patterns.

Splicing Pattern		Function annotation	Observed[1]	All[2]	*p*-value[3]	Adjust *p*-value[4]
CL6	GO	nervous system development	16	64	3.98E-03	8.05E-02
		mating	3	0	1.06E-03	6.44E-02
		synaptogenesis	4	4	5.32E-03	8.80E-02
		neuromuscular process	4	4	5.32E-03	8.80E-02
		suckling behavior	3	0	1.06E-03	6.44E-02
		mating behavior	3	0	1.06E-03	6.44E-02
		behavior	7	13	2.39E-03	8.05E-02
		learning	3	1	3.93E-03	8.05E-02
		actin filament-based movement	3	1	3.93E-03	8.05E-02
		feeding behavior	3	1	3.93E-03	8.05E-02
		anatomical structure development	23	107	2.51E-03	8.05E-02
CL7	KEGG	Endocytosis	3	14	5.26E-02	5.26E-02
		Oocyte meiosis	3	5	5.78E-03	1.16E-02
CL8	GO	cell adhesion	5	43	1.66E-02	6.08E-02
		actin cytoskeleton organization	5	38	1.04E-02	4.94E-02
		cytoskeleton organization	6	55	1.08E-02	4.94E-02
		interspecies interaction between organisms	4	15	2.55E-03	2.63E-02
		cell death	6	45	4.35E-03	2.87E-02
		apoptosis	6	34	1.17E-03	2.12E-02
		anti-apoptosis	3	5	1.61E-03	2.12E-02
		negative regulation of apoptosis	4	11	9.80E-04	2.12E-02
		death	6	45	4.35E-03	2.87E-02
		regulation of apoptosis	5	28	3.19E-03	2.63E-02
		regulation of synaptic transmission	3	12	1.12E-02	4.94E-02
		negative regulation of programmed cell death	4	11	9.80E-04	2.12E-02
		regulation of programmed cell death	5	28	3.19E-03	2.63E-02
		regulation of cellular component organization	5	47	2.31E-02	8.01E-02
		regulation of neurogenesis	3	10	7.37E-03	4.05E-02
		actin filament-based process	5	40	1.26E-02	5.21E-02
		programmed cell death	6	35	1.34E-03	2.12E-02
		negative regulation of cellular process	7	68	7.36E-03	4.05E-02
		biological adhesion	5	43	1.66E-02	6.08E-02
	KEGG	MAPK signaling pathway	3	17	2.06E-02	2.06E-02
		Focal adhesion	3	11	7.24E-03	1.45E-02

[1]*Observed:* number of genes that overlap between specific gene set and genes for segments within cluster.
[2]*All:* number of genes that overlap between specific gene set and genes for all age-related segments.
[3]*p-value:* hypergeometric test p-value.
[4]*Adjust p-value:* hypergeometric test p-value after Benjamini-Hochberg correction for multiple testing.

Table S9. List of correlated splicing factors.

Splicing Pattern	Positive correlated		Negative correlated	
	Ensemble ID	**HGNC ID**	**Ensemble ID**	**HGNC ID**
CL1	ENSG00000117569	*PTBP2*	ENSG00000100650	*SRp40*
	ENSG00000011304	*PTBP1*	ENSG00000126945	*hnRNPH2*
	ENSG00000161547	*SC35*		
	ENSG00000136527	*Tra2beta*		
	ENSG00000135486	*hnRNPA1*		
	ENSG00000096746	*hnRNPH3*		
	ENSG00000169813	*hnRNPHF*		
	ENSG00000169045	*hnRNPH1*		
CL2			ENSG00000161547	*SC35*
CL3	ENSG00000117569	*PTBP2*		
	ENSG00000048740	*ETR3*		
CL4			ENSG00000152601	*MBNL1*
CL5			ENSG00000136527	*Tra2beta*
CL6	ENSG00000126945	*hnRNPH2*	ENSG00000112081	*SRp20*
			ENSG00000096746	*hnRNPH3*
			ENSG00000169813	*hnRNPHF*
			ENSG00000169045	*hnRNPH1*
CL7	ENSG00000161547	*SC35*		
	ENSG00000100650	*SRp40*		
CL8			ENSG00000112531	*QKI*
			ENSG00000117569	*PTBP2*
			ENSG00000011304	*PTBP1*

Table S10. Enrichment of genes with cell-type specific expression in splicing patterns (top) or brain region-specific genes (bottom).

	Neurons	OPCs	OLs	Astrocytes	White matter	Gray matter
Splicing patterns						
c1	1.04	1.19	0.91	0.88	1.08	0.79
c2	1.08	0.70	1.01	0.92	1.05	0.87
c3	1.15	0.81	0.82	0.91	0.95	1.15
c4	0.94	0.29	1.23	1.29	0.98	1.05
c5	1.06	2.74	0.59	0.39	0.60	2.13
c6	0.66	0.00	1.66	1.69	0.74	1.74
c7	1.13	1.47	0.63	0.83	1.01	0.96
c8	0.57	0.00	2.53	0.83	0.75	1.70
Gene with brain region-specific expression						
PFC-specific	1.16	0.76	0.98	0.96	1.02	0.95
CBC-specific	0.80	1.31	1.03	1.05	0.95	1.11

p-value	≥0.1	≥0.05	≥0.01	<0.01

Numbers are odd ratios (observed to expected), *p*-values from Fisher's exact test are shown in different colors: ≥0.1 – white; 0.05-0.1 – light gray; 0.0-0.05 – gray; <0.01 – dark gray.

Table S11. Splicing factor binding motifs.

SFBM ID	Splicing factors		Motif feature	Reference
	Ensemble Gene ID	HGNC ID		
SF2ASF.1	ENSG00000136450	*SF2ASF*	C[AG][CG][AC][CG]G[AT]	sfmap.technion.ac.il
SF2ASF.2	ENSG00000136450	*SF2ASF*	TG[AG][AT]G[ACG][ACT]	sfmap.technion.ac.il
9G8.1	ENSG00000115875	*9G8*	ACGAGAGA[CT]	sfmap.technion.ac.il
9G8.2	ENSG00000115875	*9G8*	[AT]GGAC[AG]A	sfmap.technion.ac.il
SC35.1	ENSG00000161547	*SC35*	G[AG][CT][CT][AC]C[CT][AG]	sfmap.technion.ac.il
SC35.2	ENSG00000161547	*SC35*	TGC[CT]G[CT][CT]	sfmap.technion.ac.il
Tra2alpha	ENSG00000164548	*Tra2alpha*	GAAGAGGAAG	sfmap.technion.ac.il
Tra2beta.1	ENSG00000136527	*Tra2beta*	GAAGAA	sfmap.technion.ac.il
Tra2beta.2	ENSG00000136527	*Tra2beta*	G[ACT][ACG][ACG]GA[ACGT][AG]	sfmap.technion.ac.il
Tra2beta.3	ENSG00000136527	*Tra2beta*	AAGTGTT	sfmap.technion.ac.il
SRp20.1	ENSG00000112081	*SRp20*	CTC[GT]TC[CT]	sfmap.technion.ac.il
SRp20.2	ENSG00000112081	*SRp20*	[AT]C[AT][AT]C	sfmap.technion.ac.il
SRp40	ENSG00000100650	*SRp40*	[CT][CT][AT]C[AT][CG]G	sfmap.technion.ac.il
SRp55	ENSG00000124193	*SRp55*	[CT][AG]C[AG][GT][AC]	sfmap.technion.ac.il
hnRNPA1.1	ENSG00000135486	*hnRNPA1*	TAGACA	sfmap.technion.ac.il
hnRNPA1.2	ENSG00000135486	*hnRNPA1*	TAGAGT	sfmap.technion.ac.il
hnRNPA1.3	ENSG00000135486	*hnRNPA1*	TAGGG[AT]	sfmap.technion.ac.il
hnRNPAB	ENSG00000197451	*hnRNPAB*	ATAGCA	sfmap.technion.ac.il
hnRNPH/F.1	ENSG00000169045	*hnRNPH1*	GGCGG	sfmap.technion.ac.il
hnRNPH/F.1	ENSG00000126945	*hnRNPH2*	GGCGG	sfmap.technion.ac.il
hnRNPH/F.1	ENSG00000169813	*hnRNPHF*	GGCGG	sfmap.technion.ac.il
hnRNPH/F.2	ENSG00000169045	*hnRNPH1*	GGGTG	sfmap.technion.ac.il
hnRNPH/F.2	ENSG00000126945	*hnRNPH2*	GGGTG	sfmap.technion.ac.il
hnRNPH/F.2	ENSG00000169813	*hnRNPHF*	GGGTG	sfmap.technion.ac.il
hnRNPH/F.3	ENSG00000169045	*hnRNPH1*	TGTGGG	sfmap.technion.ac.il
hnRNPH/F.3	ENSG00000126945	*hnRNPH2*	TGTGGG	sfmap.technion.ac.il
hnRNPH/F.3	ENSG00000169813	*hnRNPHF*	TGTGGG	sfmap.technion.ac.il
hnRNPH/F.4	ENSG00000169045	*hnRNPH1*	TTGGGT	sfmap.technion.ac.il
hnRNPH/F.4	ENSG00000126945	*hnRNPH2*	TTGGGT	sfmap.technion.ac.il
hnRNPH/F.4	ENSG00000169813	*hnRNPHF*	TTGGGT	sfmap.technion.ac.il
MBNL1	ENSG00000152601	*MBNL1*	[TC]GCT[TG][TC]	sfmap.technion.ac.il
NOVA	ENSG00000139910	*NOVA1*	[TC]CA[TC]	sfmap.technion.ac.il
NOVA	ENSG00000104967	*NOVA2*	[TC]CA[TC]	sfmap.technion.ac.il
PTB.1	ENSG00000011304	*PTBP1*	CTCTCT	sfmap.technion.ac.il
PTB.2	ENSG00000011304	*PTBP1*	TCTT	sfmap.technion.ac.il
PTB.1	ENSG00000117569	*PTBP2*	CTCTCT	sfmap.technion.ac.il
PTB.2	ENSG00000117569	*PTBP2*	TCTT	sfmap.technion.ac.il
CUG-BP	ENSG00000149187	*CUG-BP*	TGCTG	sfmap.technion.ac.il
YB1	ENSG00000065978	*YB1*	CAACCACAA	sfmap.technion.ac.il
FOX1	ENSG00000078328	*FOX1*	TGCATG	sfmap.technion.ac.il
QKI.1	ENSG00000112531	*QKI*	ACTAA[TC].{1,30}A[TC]	[1]
QKI.2	ENSG00000112531	*QKI*	TAA[TC].{1,30}ACTAA[TC]	[1]
ETR3	ENSG00000048740	*ETR3*	TGTGTG	[2]
HuD.1	ENSG00000162374	*HuD*	[CG][CT][CT]TC[CT][CT]TC[TC]C[TC]C	[3]
HuD.2	ENSG00000162374	*HuD*	[TG]TTTGTTT[TG][GT]TTT	[3]
HuD.3	ENSG00000162374	*HuD*	TTTTTTTTT[TA]AAA	[3]
SFRS1	ENSG00000136450	*SFRS1*	GAAGAA	[4]

Table S12. PCR primers.

Gene and relative segment location[1] (bp)	Up-stream primer sequence (5'-3')	Down-stream primer sequence (5'-3')	Product lengths (bp) (long/short)
AGAP3 34157-37048	TCAGCGACTACTCGTCCTCAG	AGTTGGAAACAGTGGCACAT	380/154
AKR1B1 11261-11987	GCAGCCAAGCACAATAAAACT	ATCACCACCAAGTTCCTCTG	699/71
ASPH 181884-181928	AAGAATGGGAGGAAAGGC	ACTTTGGCATCATCCACATC	236/191
CADPS 83378-83510	ATGTGGATCTGATGGAGTCC	GTCCCGAATGAAGGTCTG	290/143
CDC42BPA 21014-21199	GCTACGAGATCCAGAAATG	GGAATACTGACTGAGCCACT	351/165
CTNNA2 1433854-1433997	AAGGTGAAGGCAGAAGTG	CTGGTATTTGGTTGAGGC	294/150
DBN1 2996-3133	TGACAACCCAAGGGAGTTCT	GCTCTATCTGCTCAGCGACAG	334/196
DCLK1 19228-19301	CAAGCCGAATAGCACAGC	TTCCGATTCCGAGTTGAG	225/151
EXD3 56722-66995	GCTTTGACATCAAGGACG	CTCCTGCAGACGCAAGAC	1125/107
FMNL2 305555-313054	CAAAGAGGCAGCAGCAAG	TGGGCAGTTTCATTCACG	396/270
GRIN1 9763-9825	CCTACTCCCACCAGTCCAG	TCTTTCGCCTCCATCAGC	274/211
LMO7 234827-234935	TTGGAGACAGCCTCCTTG	TGCAGTACAGTTGGTGGTTT	443/334
MAPRE3 53642-53686	GACGCAAACTATGATGGAAAG	TGGGCATCAGTCTCATGG	257/212
MAPT 115927-116019	AGAAGGTGGCAGTGGTCC	ATGGATGTTGCCTAATGAGC	320/227
MAPT 77476-77535	AAGAGGGTGACACGGACGCT	TTGCTGGAATCCTGGTGGC	330/243
MATR3 51545-51688	TTAGGTGATGTGGCTTCT	AAGTTCCTCGATCTTGTC	264/120
NDRG2 6102-6143	GGTGCAGATCACAGAGGAG	ACATCGTGGTAGGTAAGGAT	195/153
NEO1 240857-241015	GTCTACACTGGCTGGAAG	ATGTTTGAGACGAAGAGG	288/129
NRCAM 78008-78064	ATACTCAAACCATACAGCAG	CTCCAGTGAAAGCACATT	203/146
PALM 31400-31531	ACAAGCGAGTCTCCAACAC	GCTTTGTGGATGAGTTCG	274/142
R3HDM1 73402-90154	CAATGAAGGATTTGGAGG	ACTTATCACTGGCCTTTTC	351/219
SGIP1 148487-148911	GCTACCCCACCCCGAAC	TGCAAGCAACCAAAGGAG	589/88
UBP1 47918-48809	TAATCAGGTTTACAGACAG	TAAAAAACAACTCTCATCTT	788/91
WNK1 126651-127109	CACTTTCACAGACATCAACCT	AGTGGTCGGCTGGGTAG	917/179

[1]Relative segment location is counted from the 5' end of each gene.

Supplementary figures

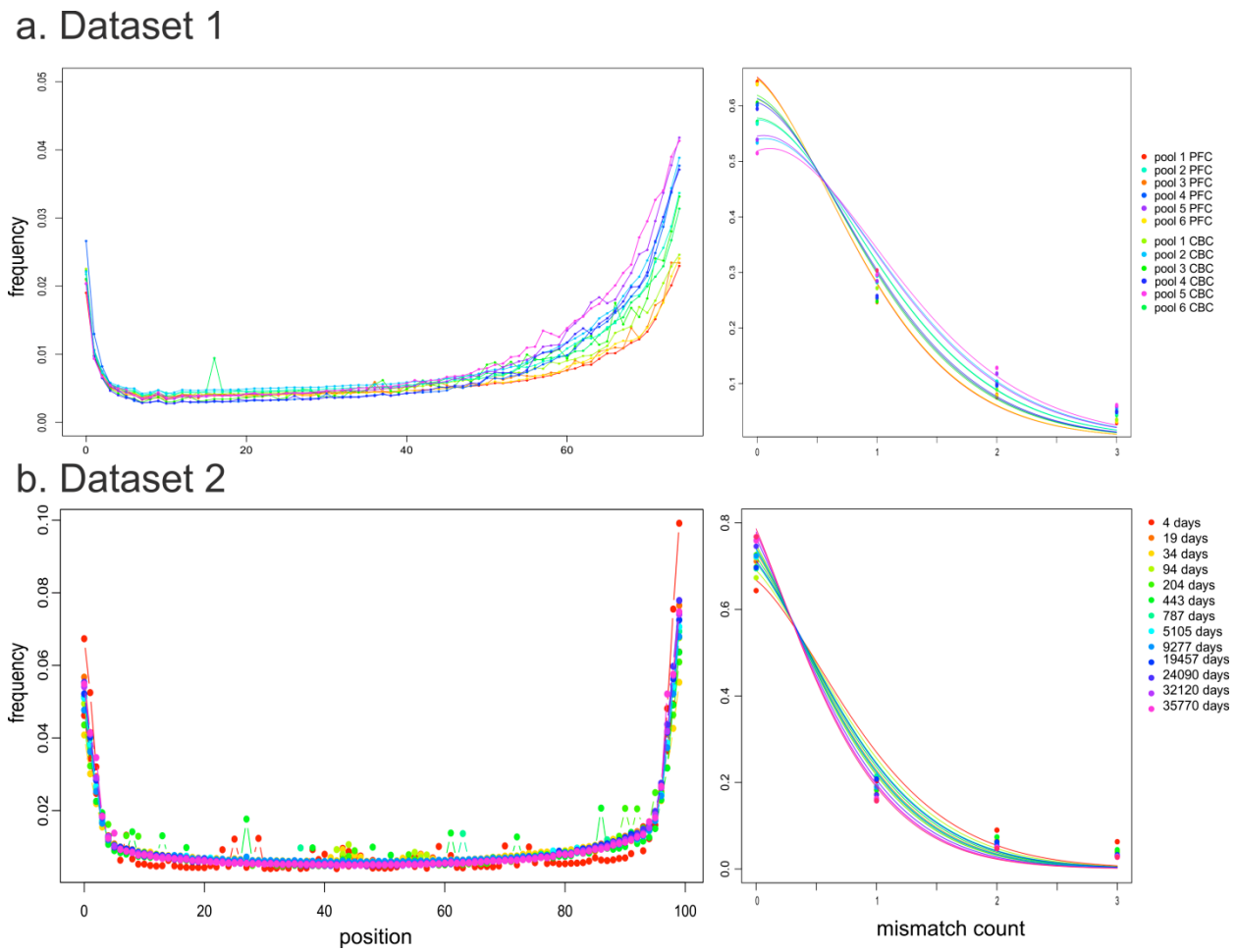

Figure S1. The distribution and frequency of mismatches along reads.

In the left panel, the x-axis shows the nt position within read (from 0 to 75 for DS1, or from 0 to 100 from DS2) and the y-axis shows the proportion of mismatches occurring at a given position. In the right panel, the x-axis shows the mismatch count (maximum of three mismatches were allowed by the mapping procedure), the y-axis shows frequency of reads with a given number of mismatches. The curves represent a fitted Poisson distribution.

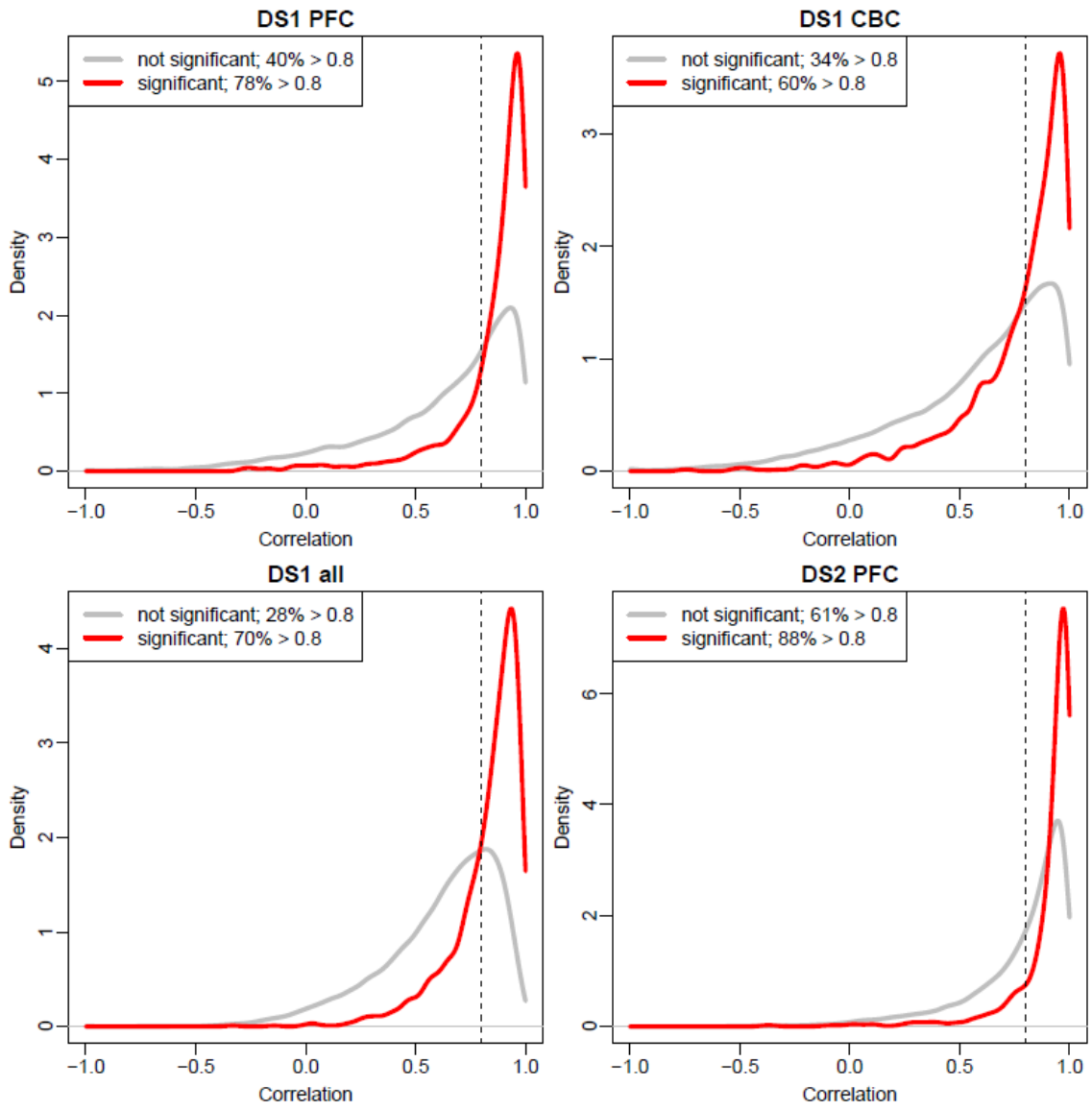

Figure S2. Effect of allowing mismatches during read mapping on inclusion ratio changes with age.

Shown are distributions of Pearson correlation coefficient between inclusion ratio changes with age calculated based on reads mapped allowing up to three mismatches and reads mapped allowing zero mismatch. Correlation coefficient distributions are plotted for 1,484 segments with significant age-related splicing changes with age (red) and 28,638 remaining segments with sufficient reads coverage (gray). The vertical dashed line indicates r=0.8 cutoff. The percentage of segments with correlation coefficient greater than 0.8 is shown in the plot legend.

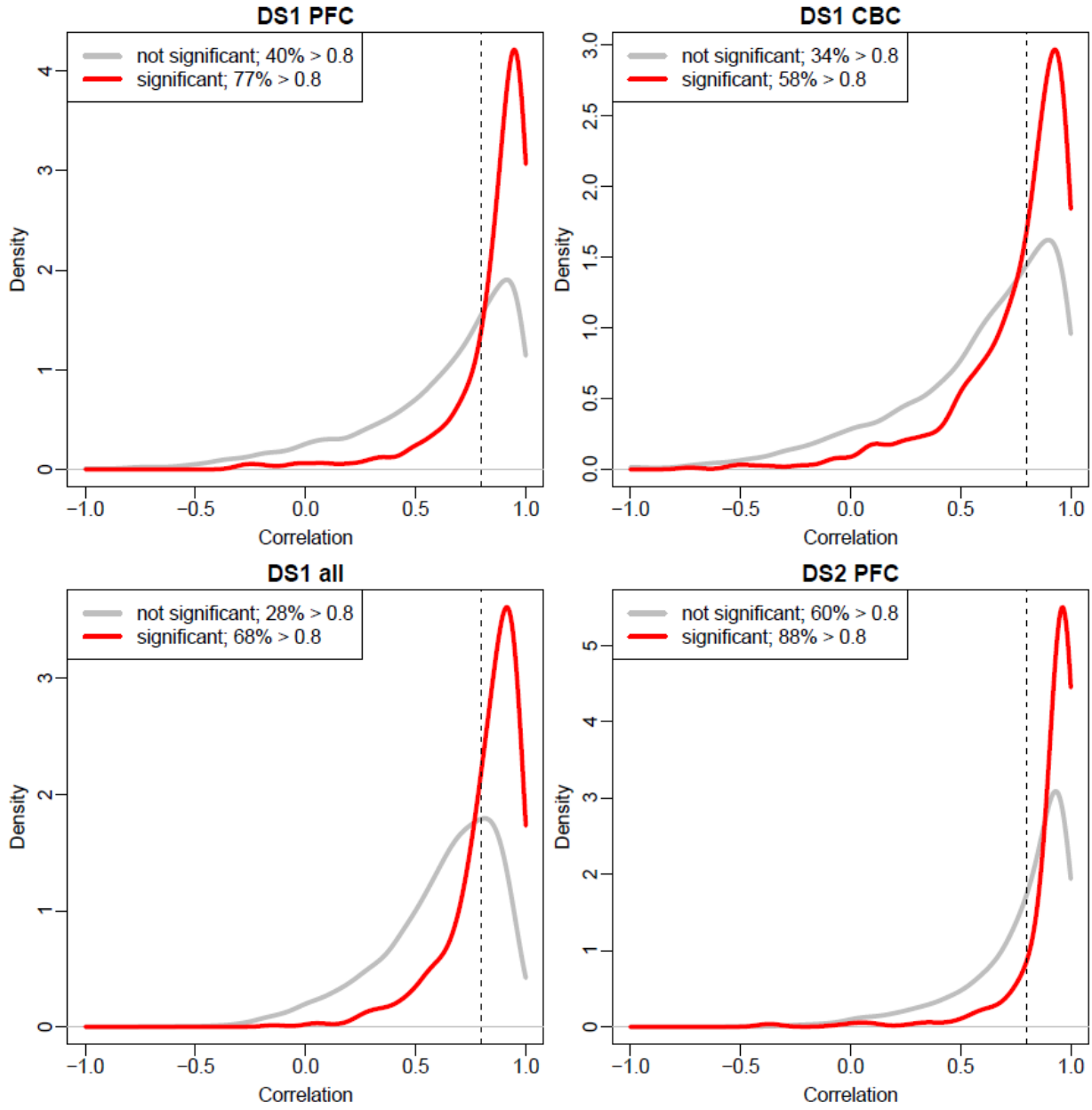

Figure S3. Effect of allowing mismatches during read mapping on changes in intron retention with age.

Shown are distributions of Pearson correlation coefficient between inclusion ratio changes with age calculated based on reads mapped allowing up to three mismatches and reads mapped allowing zero mismatch. Correlation coefficient distributions are plotted for 620 retained introns with significant age-related splicing changes with age (red) and 11,999 remaining retained introns with sufficient reads coverage (gray). The vertical dashed line indicates r=0.8 cutoff. The percentage of retained introns with correlation coefficient greater than 0.8 is shown in each panel's legend.

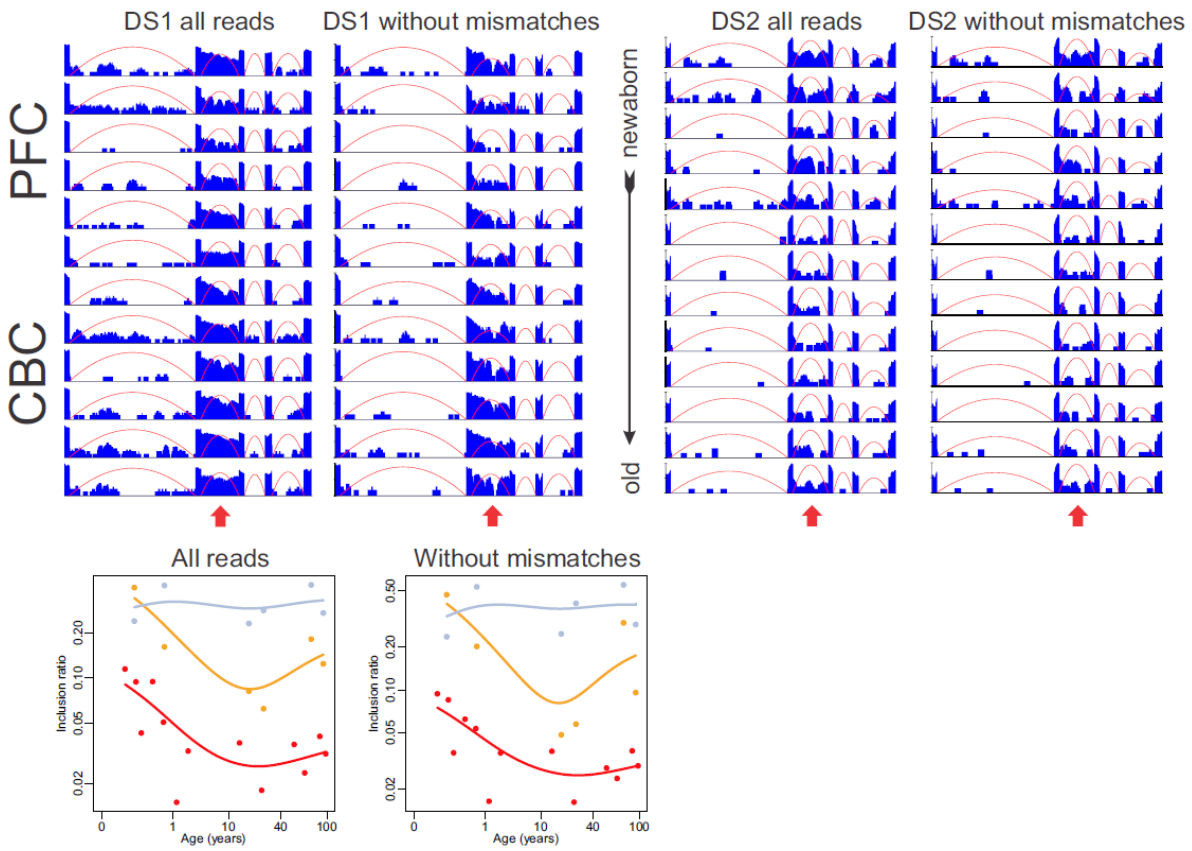

Figure S4. Retention of the 7th intron of the *AKR1B1* gene.

Top: RNA-seq coverage plots of the *AKR1B1* gene based on DS1 (left) and DS2 (right) data. The reads coverage is shown for all reads mapped with up to three mismatches allowed (all reads), and only for reads mapped with zero mismatches (without mismatches). Numbers of reads mapped to a genomic location are shown in blue, red arcs represents reads mapped to exon-exon junctions. RNA-seq coverage and inclusion ratio profiles are shown on log scale. The retained intron (the 7th intron of the gene) is indicated by the red arrow.

Bottom: inclusion ratio profiles of intron 7 of the *AKR1B1* gene. Each dot represents one sample, DS1 PFC, DS1 CBC and DS2 PFC are shown in orange, gray and red respectively, curves are cubic splines with three degrees of freedom.

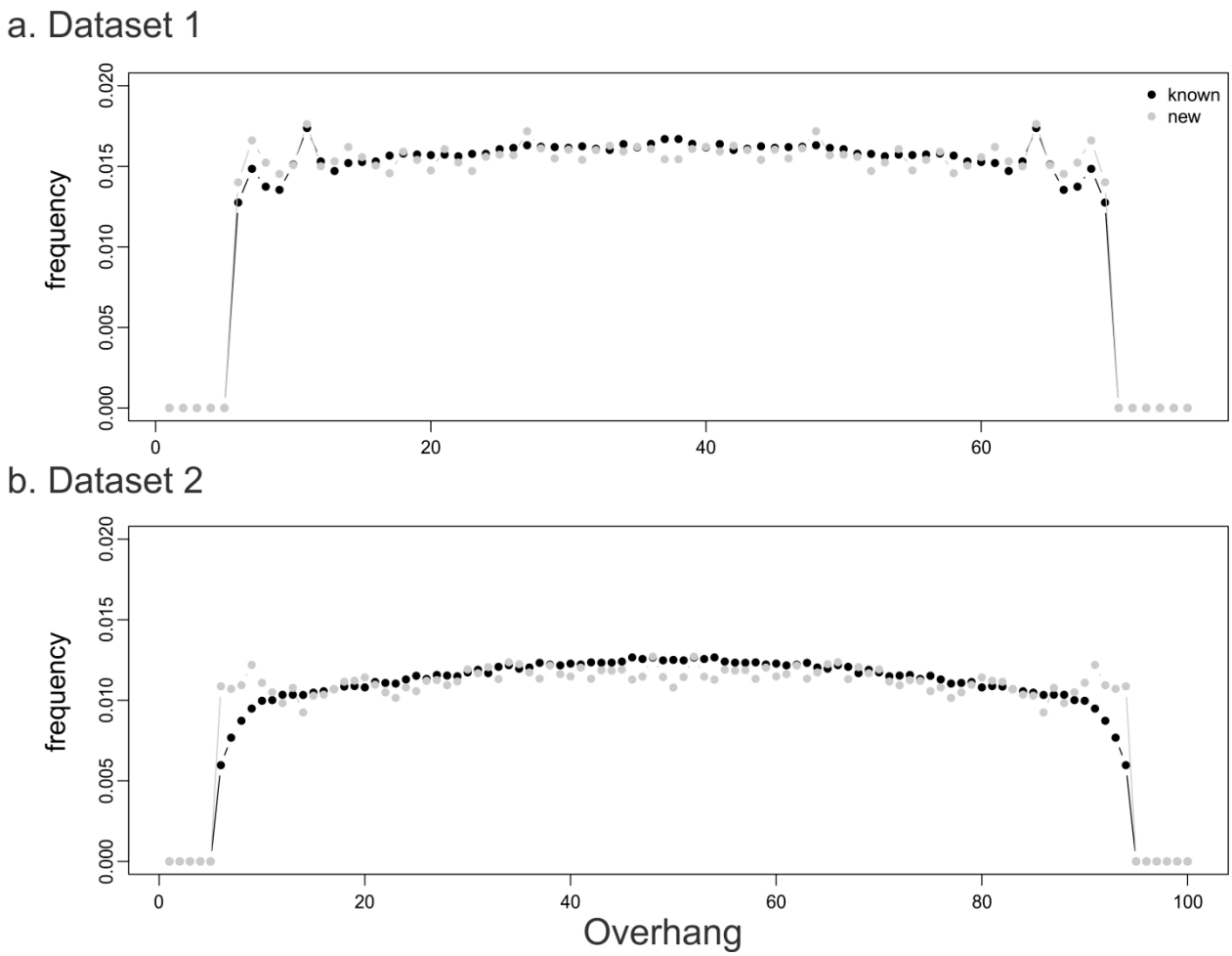

Figure S5. The distribution of read overhangs lengths spanning splice junctions.

Distribution of read overhangs (part of a read belonging to one exon) for reads mapped across splice junctions that consist of two exons and confirmed by at least two (DS1) or at least four (DS2) independent reads (reads with different mapping positions). Distribution of overhang length for reads spanning annotated junctions is shown in black, for reads spanning new junctions - in gray. Overhangs shorter than 6 nt were not considered. The x-axis shows the overhang length (nt).

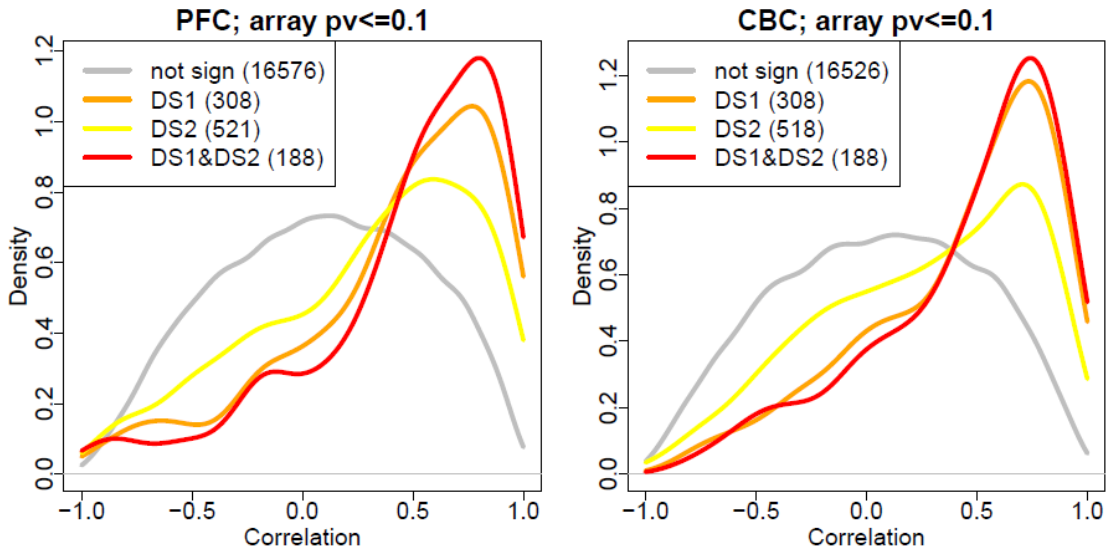

Figure S6. Correlation between age-related inclusion ratio changes measured by Affymetrix Exon Arrays and RNA-seq.

Shown are the correlations of the age-related inclusion ratio changes measured by RNA-seq (DS1) and Exon Arrays in CBC (right) and PFC (left) for segments with no significant age-related splicing change in the RNA-seq data (gray); segments significant only in the DS1 (orange); segments significant only in the DS2 (apricot), and segments significant in both datasets (red). Only segments showing significant age-related inclusion ratio trend (permutations, $p<0.1$) in the Exon Array dataset were used in analysis.

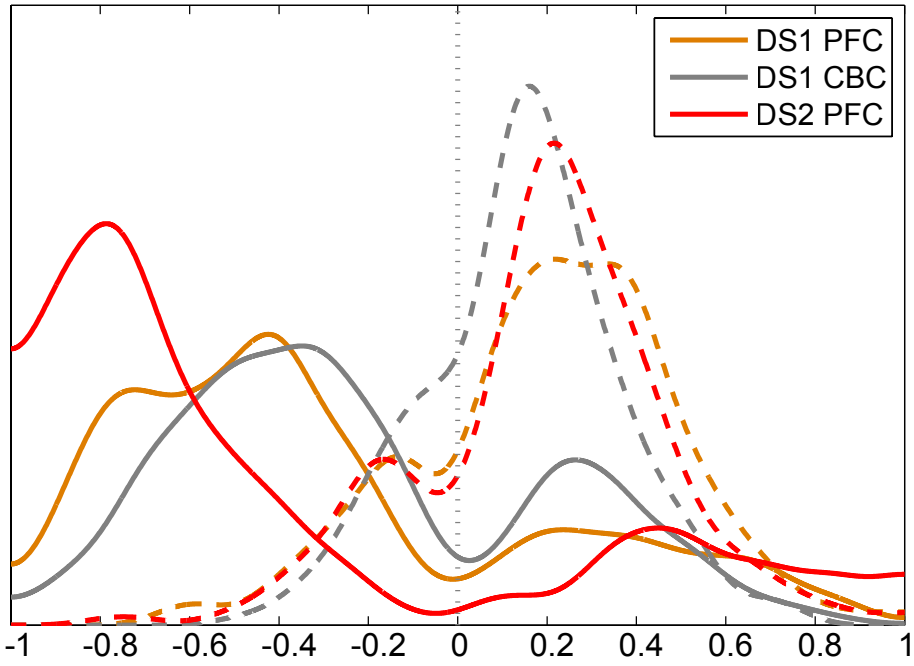

Figure S7. Inclusion ratio change index distribution for gene segments showing significant inclusion ratio change in development and/or aging.

Shown are developmental inclusion ratio change index distributions based on 970 segments showing significant splicing changes in development (solid lines) and aging inclusion ratio change index distributions based on 310 segments showing significant splicing changes in aging (dashed lines). Splicing changes in development and aging were identified using a linear model analysis based on five samples with ages between 2 days and 25 years for development, and five samples with ages between 25 years and 100 years for aging. All samples were selected from 13 individuals constituting DS2 (Supplementary Table S2). The 970 and 310 segments were identified among 1,484 segments with significant age-related splicing changes over the entire lifespan.

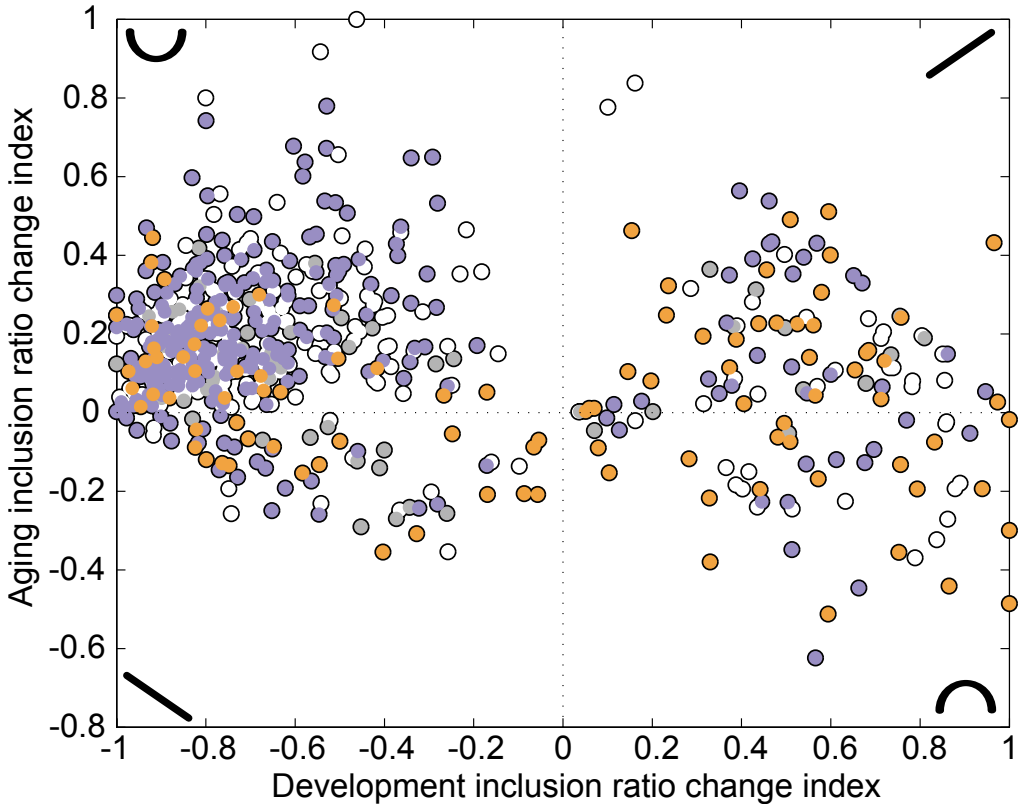

Figure S8. Scatter plot of splicing change index distribution containing splicing type information.

Shown are inclusion ratio change index distributions based on 659 segments showing significant splicing changes in development and/or aging among 1,484 segments with significant age-related splicing changes over the entire lifespan. As an additional criterion, segments were required to show consistent age-related change between DS1 and DS2 in both time intervals. The inclusion ratio change indexes shown were calculated based on DS2. The colors show different splicing types: violet – skipped exons, yellow – retained introns, gray and white – complex and mixed splice types. The four quadrants of the plot correspond to four patterns of inclusion ratio change with age: down-up, up-up, up-down and down-down as indicated by the black pattern diagrams shown in the four corners of the plot.

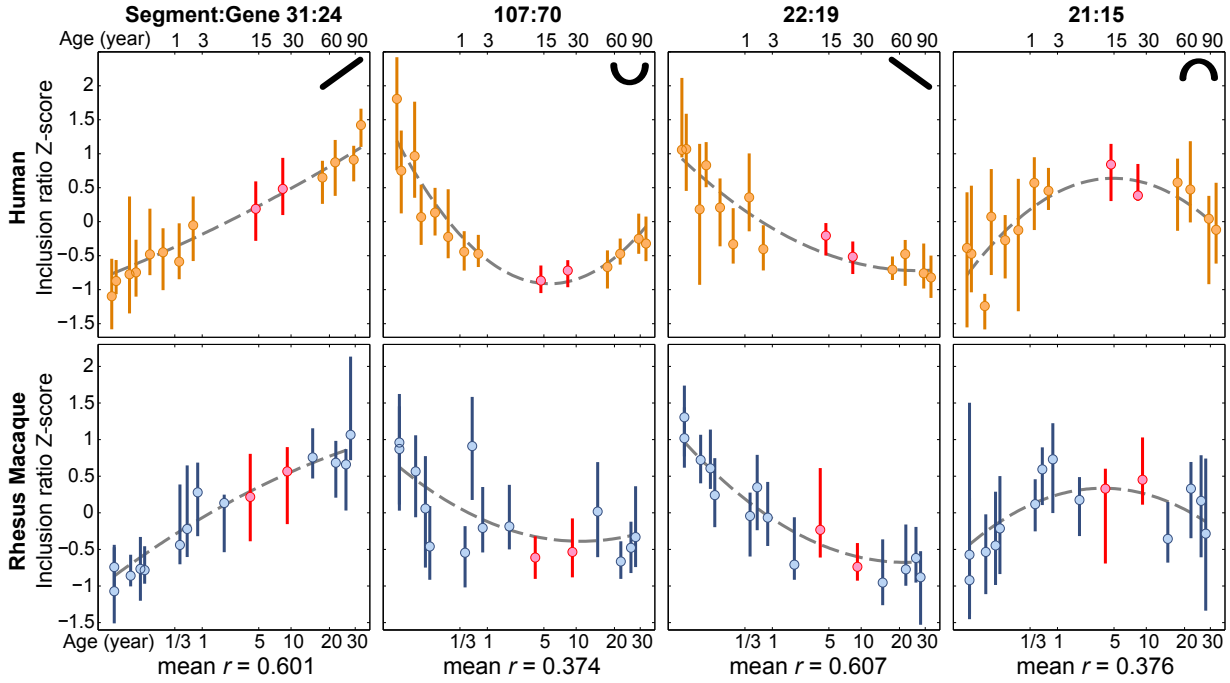

Figure S9. For major age-related splicing change patterns in the human and macaque PFC.

The panels show trajectories of splicing changes with age in the human (upper panels) and rhesus macaque (lower panels) PFC sorted according to the four major patterns depicted in the upper right corner of the upper panels. The changes are drawn for a total of 181 segments showing significant age-related changes in the human or macaque PFC and showing consistent splicing change direction in the two human datasets (DS1 and DS2). Correlations between the human and the macaque trajectories of splicing changes with age were robust with regard to segments selection criteria: All four main splicing patterns showed significantly greater positive correlations for 496 segments identified in humans that also mapped to macaques (mean r between 0.2 and 0.5; permutation test, $p<0.05$), as well as for the 290 segments identified in the human or the macaque time series (mean r between 0.4 and 0.6; permutation test, $p<0.005$). The segments were grouped into the four patterns based on their inclusion ratio changes with age in the human PFC. The inclusion ratios were normalized to mean=0 and standard deviation=1 before plotting. The vertical lines show 25% and 75% quartiles of the inclusion ratios across segments in a group, the cycles show the median. The mid-age samples used to separate development and aging phases are shown in red. The gray dashed line represents the quadric regression curve fitted to the median values. The numbers of segments and genes in each group are labeled on the top of the panel. The mean Pearson correlation coefficients of the segments'

inclusion ratios for each of the four patterns calculated between the human and the rhesus macaque time series are shown underneath the panels.

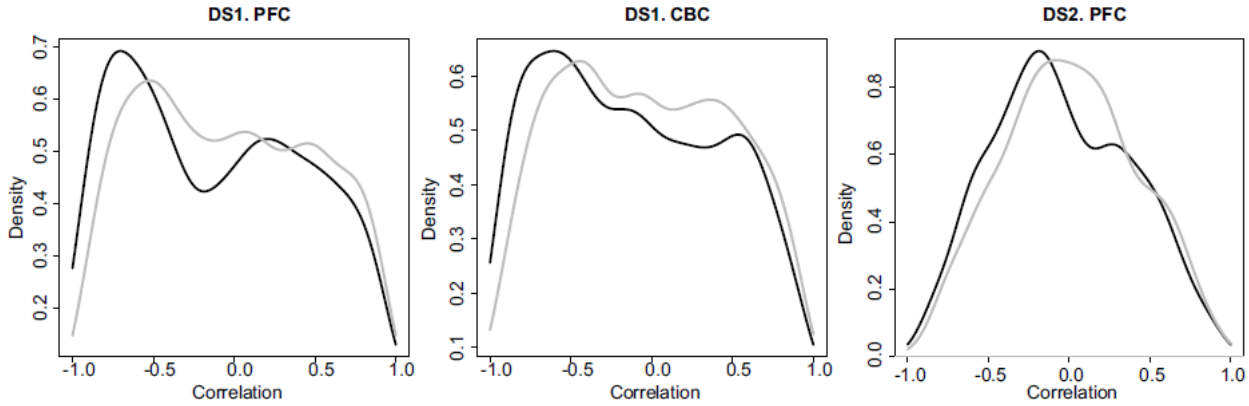

Figure S10. Relationship between gene expression and segment inclusion ratio.

Distribution of correlation coefficient between segment inclusion ratio and gene expression for segments with significant age-related splicing changes in both datasets and inclusion ratio defined in all samples (*N* = 1,422) in DS1 PFC (left), DS1 CBC (middle) and DS2. Observed distribution is shown in black, background distribution (obtained by random assignment of segments to genes) is shown in gray.

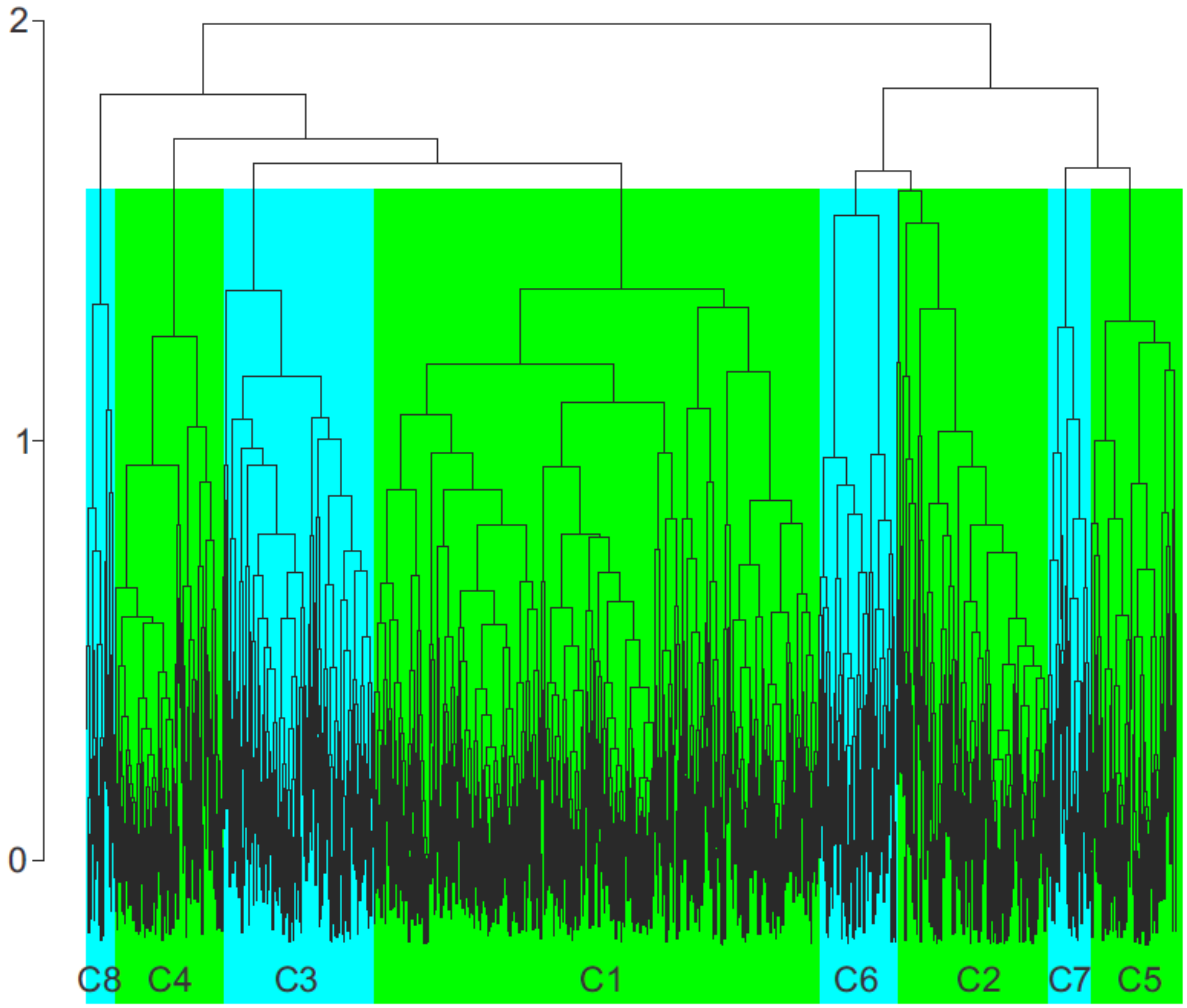

Figure S11. Hierarchical clustering of inclusion ratio values reveals distinct splicing patterns.

Hierarchical clustering dendrogram of segments with significant age-related splicing changes in both datasets and inclusion ratio defined in all samples (N = 1,422). The clustering was done using the "complete" method. As distance measure, we used the pairwise negative Pearson correlation coefficient (specifically, $1 - r$) between the inclusion ratio of segments from both brain regions. The colored areas indicate identified splicing patterns, numbered according to their size.

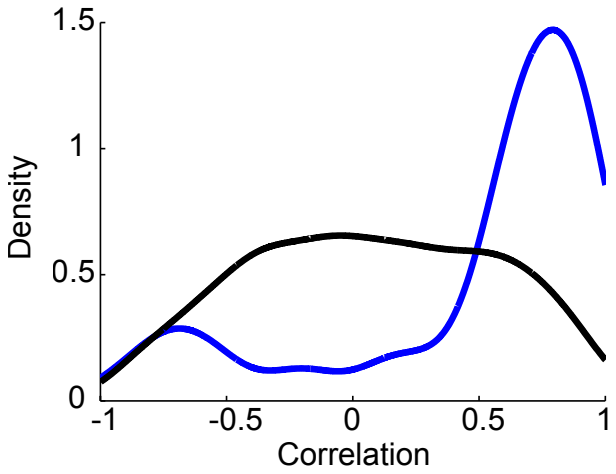

Figure S12. Correlation of differences in age-related splicing changes between PFC and CBC measured using RNA-seq and Affymetrix Exon Arrays.

Shown are the distributions of Pearson correlation coefficients based on a comparison of inclusion ratio differences between PFC and CBC measured using RNA-seq and Affymetrix Exon Arrays. This analysis is based on 601 segments showing significant age-related splicing changes in both RNA-Seq DS1 and Exon Array dataset. The blue line shows the distribution of Pearson correlation coefficients based on 71 out of 601 segments with significant differences in age-related splicing patterns between PFC and CBC in RNA-Seq. The black line shows the distributions of Pearson correlation coefficients based on the remaining 530 segments with no significant differences in age-related splicing patterns between PFC and CBC in RNA-Seq. An excess of positive correlations for segments showing significant splicing pattern differences between two brain regions is not expected, compared to the remaining segments (one-sided Wilcoxon test, $p<0.0001$), and indicates good agreement between RNA-seq and Affymetrix Exon Array platforms.

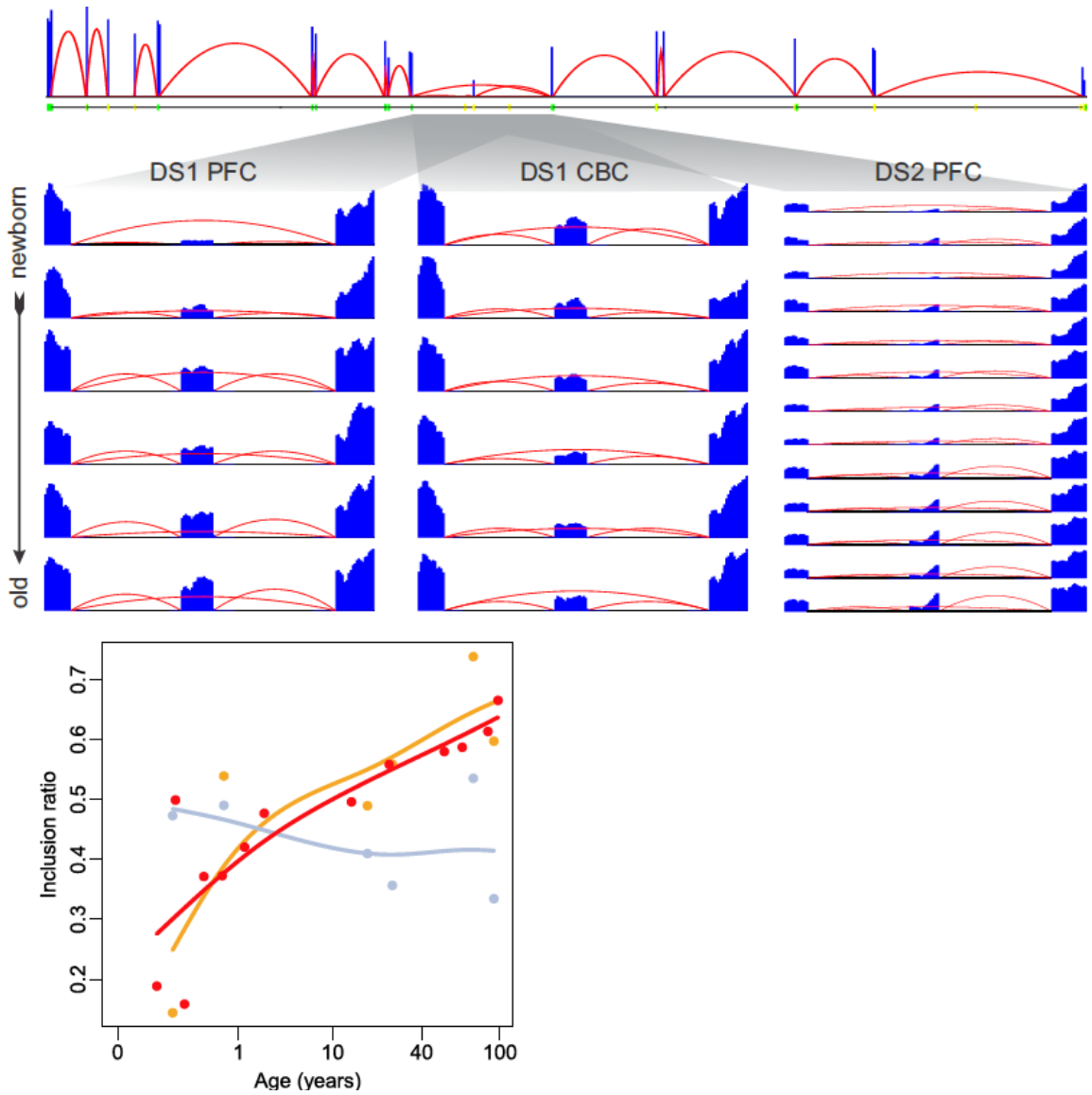

Figure S13. Alternative splicing of *APP* exon 9.

Top: RNA-seq coverage plots of the whole *APP* (amyloid beta (A4) precursor protein) gene based on all samples from DS1. A zoomed region of the 8th to 10th exons (not to scale) is also shown based on DS1 PFC (left), DS1 CBC (center) and DS2 (right) data. The reads coverage is shown for all reads mapped with up to three mismatches. Numbers of reads mapped to a genomic location are shown in blue, red arcs represents reads mapped to exon-exon junctions.

Bottom: inclusion ratio profiles of the 9th exon of the *APP* gene. Each dot represents one sample, DS1 PFC, DS1 CBC and DS2 PFC are shown in orange, gray and red respectively, curves are cubic splines with three degrees of freedom.

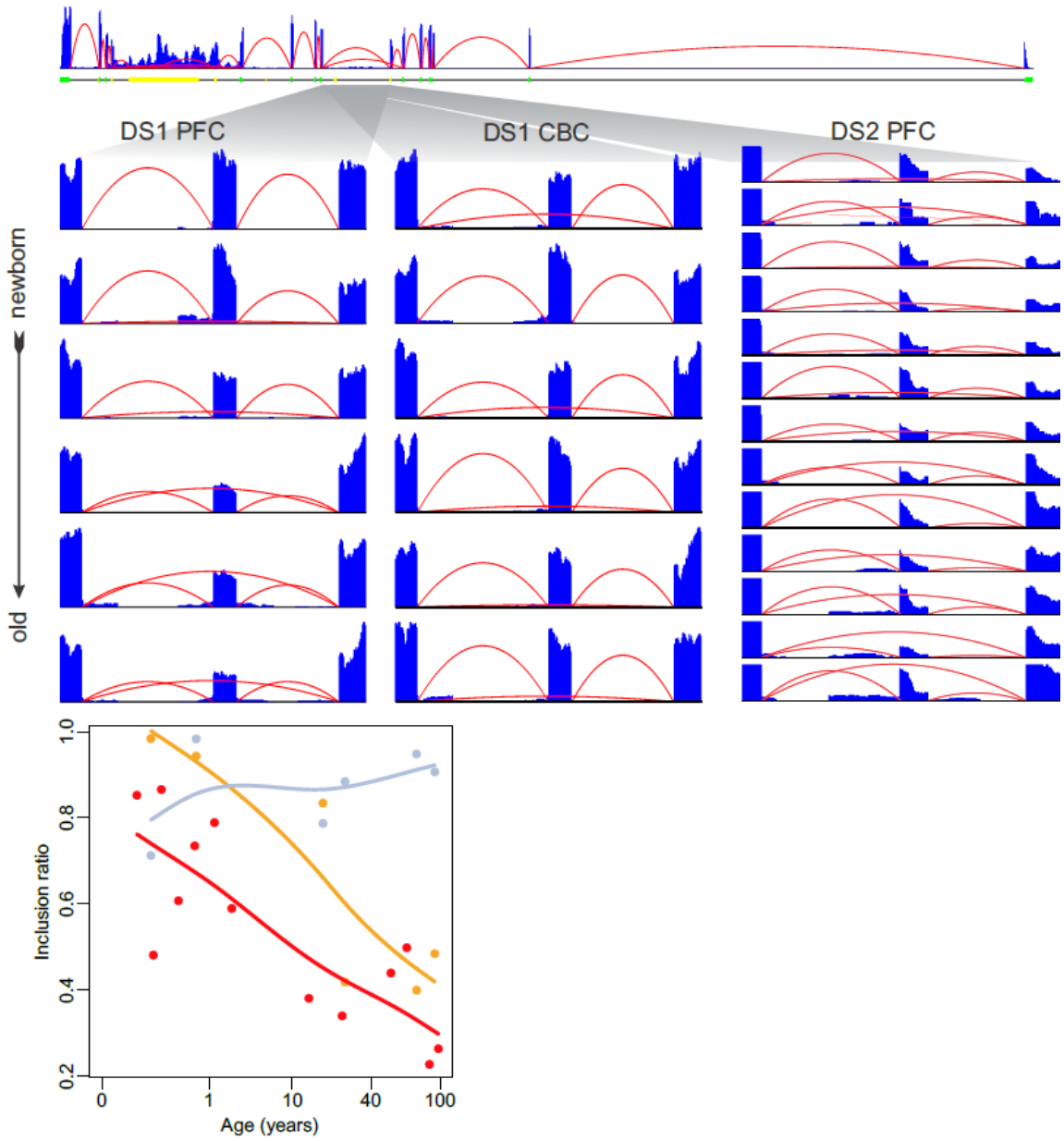

Figure S14. Alternative splicing of the 6th exon of the *BIN1* gene.

Top: RNA-seq coverage plots of the whole *BIN1* gene based on all samples from DS1. Zoomed region of 5th to 7th exons (not to scale) is also shown based on DS1 PFC (left), DS1 CBC (center) and DS2 (right) data. The reads coverage is shown for all reads mapped with up to three mismatches. Numbers of reads mapped to a genomic location are shown in blue, red arcs represents reads mapped to exon-exon junctions.

Bottom: inclusion ratio profiles of the 6th exon of the bridging integrator 1 (*BIN1*) gene. Each dot represents one sample, DS1 PFC, DS1 CBC and DS2 PFC are shown in orange, gray and red respectively, curves are cubic splines with three degrees of freedom.

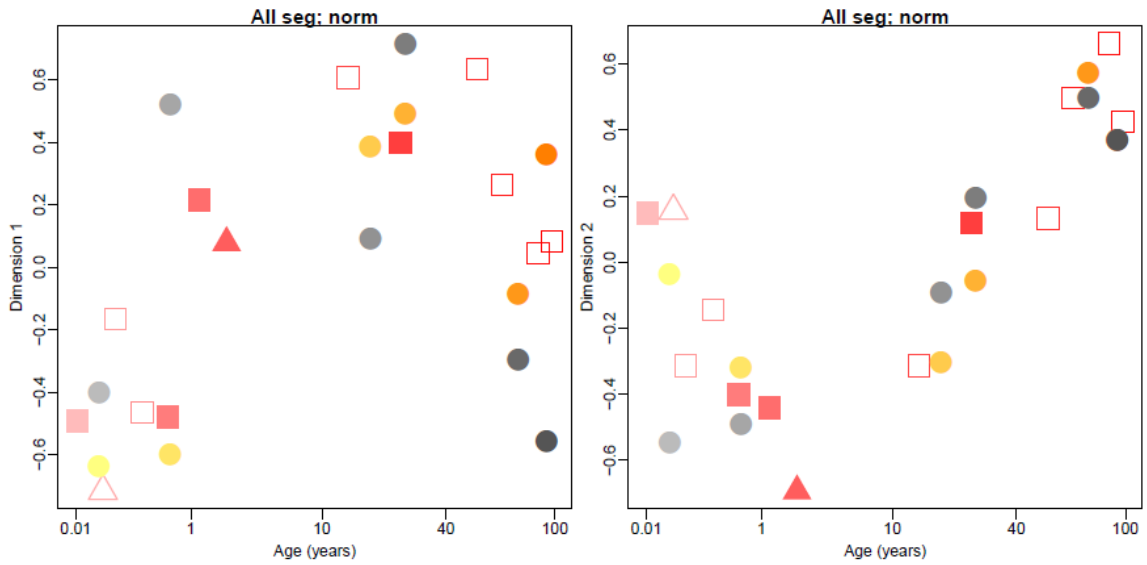

Figure S15. Multi-dimensional scaling (MDS) analysis of splicing divergence.

Shown are the results of Multi Dimensional Scaling (MDS) in two dimensions based on splicing the variation data from DS1 and DS2. Plots show the relationship between the first (left panel) and second (right panel) MDS dimensions and age. Each point represents one sample. DS1 samples are represented by cycles (PFC - orange, CBC - gray). DS2 samples are represented by triangles (women) and squares (men); filled symbols represent African Americans, empty symbols - Caucasians. For both DS1 and DS2 darker colors correspond to older age. The analysis is based on 30,122 segments with sufficient sequence read coverage in both datasets.

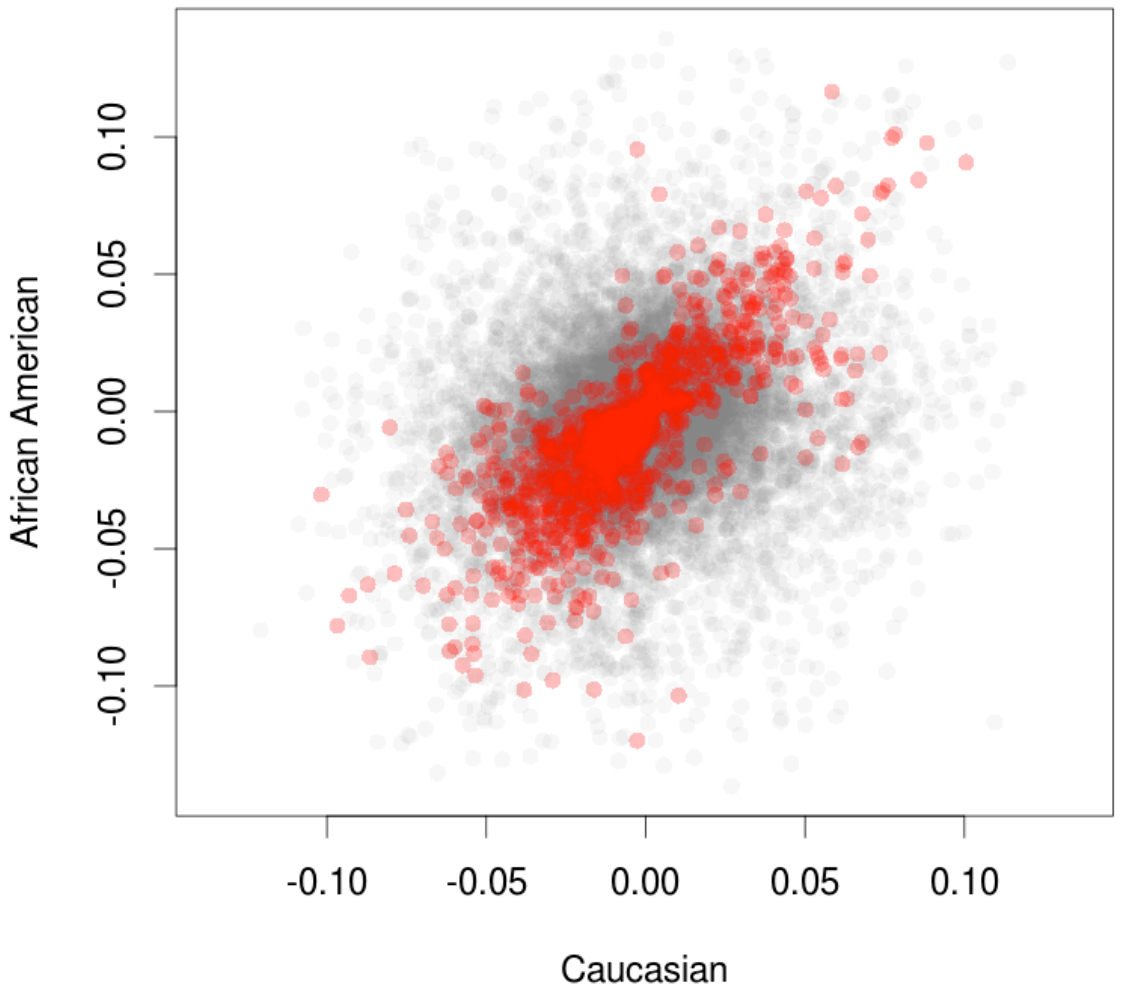

Figure S16. Age-related splicing changes in African-Americans and Caucasians.

Plotted are the rates of age-related splicing change in five African-American (Y-axis) and five Caucasian (X-axis) samples from DS2. Positive values represent inclusion ratio increase with age, negative values represent decrease. Each point represents a segment. Data for the 1463 segments with significant age-related splicing changes, and sufficient coverage in the 10 samples used in our analysis, are shown in red, 26670 segments that are not significant are shown in gray. Pearson correlation coefficient is 0.75 for segments with significant age-related splicing changes and 0.22 for non-significant segments.

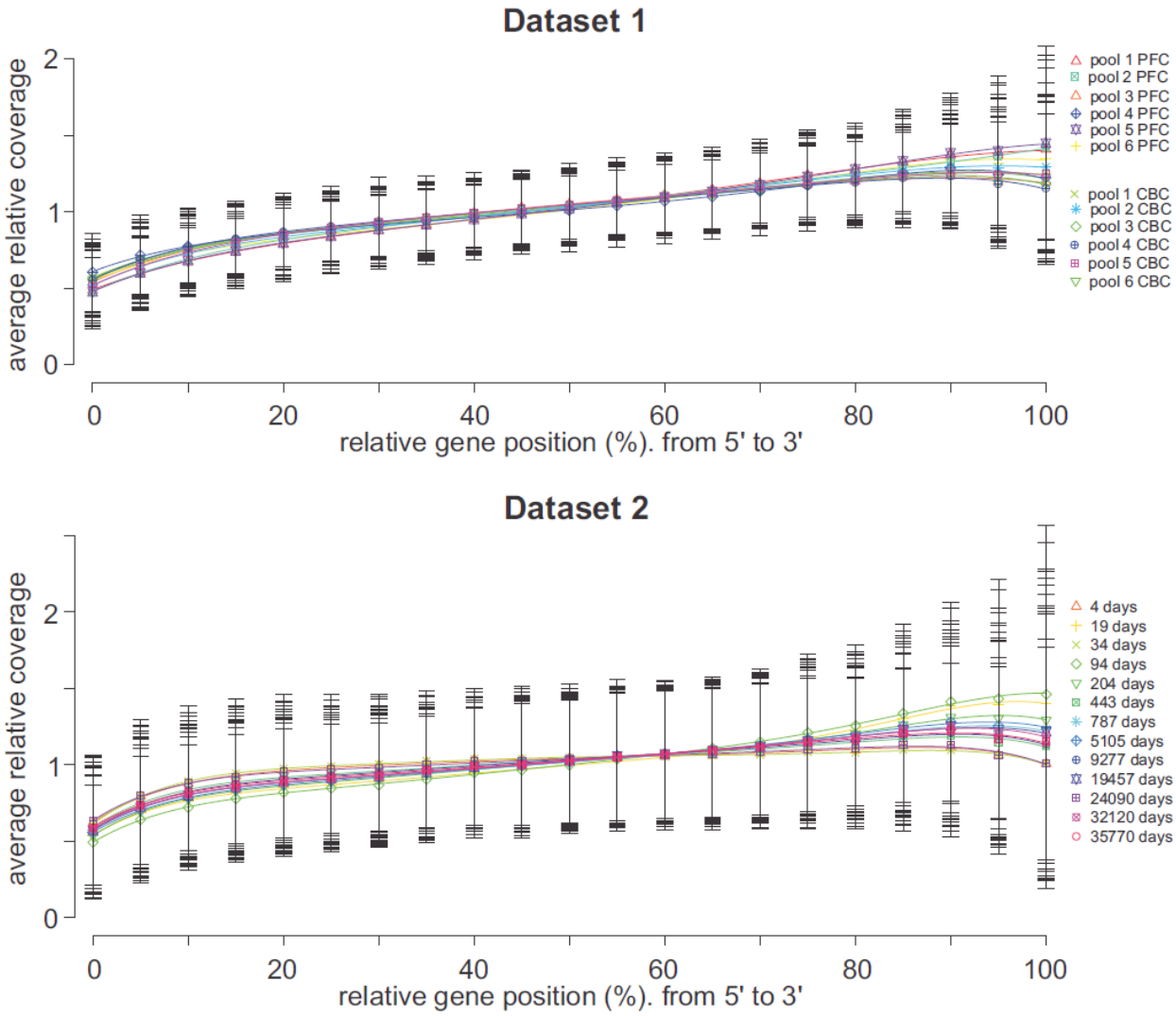

Figure S17. Gene coverage bias.

Shown are the average (among tested genes, 8,365 in DS1 and 8,061 in DS2) relative coverage of each nt binned into 21 bins along the gene. The relative coverage was defined as number of reads mapped to the nt divided by average number of read mapped to coding constitutive part of the gene. The x-axis represents relative position within transcript. Error bars represent ½ of the standard deviation.

Supplementary references

1. Galarneau A, Richard S (2005) Target RNA motif and target mRNAs of the Quaking STAR protein. Nature Structural & Molecular Biology 12: 691-698.
2. Faustino NA, Cooper TA (2005) Identification of putative new splicing targets for ETR-3 using sequences identified by systematic evolution of ligands by exponential enrichment. Molecular and Cellular Biology 25: 879-887.
3. Bolognani F, Contente-Cuomo T, Perrone-Bizzozero NI (2010) Novel recognition motifs and biological functions of the RNA-binding protein HuD revealed by genome-wide identification of its targets. Nucleic Acids Research 38: 117-130.
4. Sanford JR, Wang X, Mort M, VanDuyn N, Cooper DN, et al. (2009) Splicing factor SFRS1 recognizes a functionally diverse landscape of RNA transcripts. Genome Research 19: 381-394.